Received 26.06.26 26/8130
Revised 02.09.26

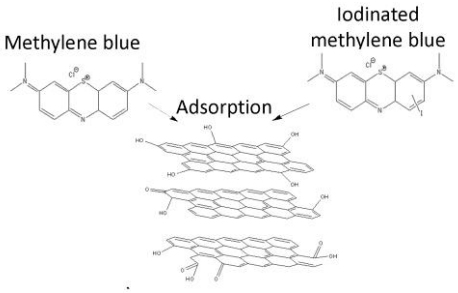
Adsorption of iodinated methylene blue on the surface of oxidized graphene nanoflakes

Evgeniya V. Suslova,*[a] Tatiana V. Vdovyi,[a] Denis M. Zakharov,[a] Denis A. Shashurin[a,b] and Georgy A. Chelkov[a,c]

[a] *Department of Chemistry, M. V. Lomonosov Moscow State University, 119991 Moscow, Russian Federation. E-mail: suslovaev@my.msu.ru*
[b] *Department of Fundamental Medicine, M. V. Lomonosov Moscow State University, 119991 Moscow, Russian Federation*
[c] *Joint Institute for Nuclear Research, 141980 Dubna, Moscow Region, Russian Federation*

DOI: 10.71267/mencom.8130

The kinetics and adsorption isotherms of iodinated methylene blue (I-MB) on the surface of oxidized graphene nanoflakes (GNFs), acting as a structural analogue of melanin, are described for the first time. The GNF adsorption capacity for I-MB (357 mg·g^{-1}) is only 5% lower than that for methylene blue (375 mg·g^{-1}), making it a promising candidate for creating selective contrast agents for visualization of melanin-containing tumors such as melanoma. The interaction mechanism between methylene blue and I-MB with GNFs is investigated and discussed.



Keywords: methylene blue, iodinated methylene blue, contrast agent, melanoma, isotherm adsorption, kinetic adsorption

Methylene blue (MB) is commonly used in surgery as a dye that selectively accumulates in specific tissues, i.e., lymph nodes and melanoma cells containing melanin.[1,2] This selectivity makes MB a promising platform for the design of selective radiopharmaceutical compounds as well as contrast agents for visualization of melanin-containing structures by other methods, for example, X-ray and computed tomography. MB itself does not have the required radiological or X-ray imaging properties, however, it can be functionalized by the introduction of heavy iodine atoms into its structure. MB functionalized with radioactive isotopes ^{123}I, ^{131}I and ^{211}At has been described as a potential radiopharmaceutical agent for radiotherapy of melanoma.[2-6] However, further research in this area, especially the development of MB-based contrast agents, requires comprehensive data on the adsorption properties of iodinated MB (I-MB) for melanin or other adsorbents with comparable structures, which are currently unavailable.

The present study was aimed at bridging this gap for the first time and was devoted to comparative analysis of the kinetics and adsorption isotherms of I-MB and MB on the surface of graphene nanoflakes (GNFs) used as a structural analogue of melanin.

Melanin is a natural polymer formed by variable phenolic or indolic structural units, whose exact structure considerably varies depending on its source.[7] It consists of extended planes with an interlayer distance of 3.4 Å that are disordered relative to each other, according to transmission electron microscopy (TEM) data (Figure 1a, d). GNFs (Figure 1b, e) and oxidized GNFs (Figure 1c, f) particles have a similar layered structure consisting of 7-10 stacked graphene sheets with a similar interlayer distance. Melanin surface contains carboxyl, hydroxyl, and amine functional groups.[7-9] Similarly, oxidized GNFs contain carboxyl and hydroxyl groups.[10] MB interacts with melanin and graphene derivatives through π-π stacking and electrostatic interactions of positively charged MB molecules and negatively charged groups in their structures.[11-13] Such similarity allows using oxidized GNFs as an accessible analogue of melanin.

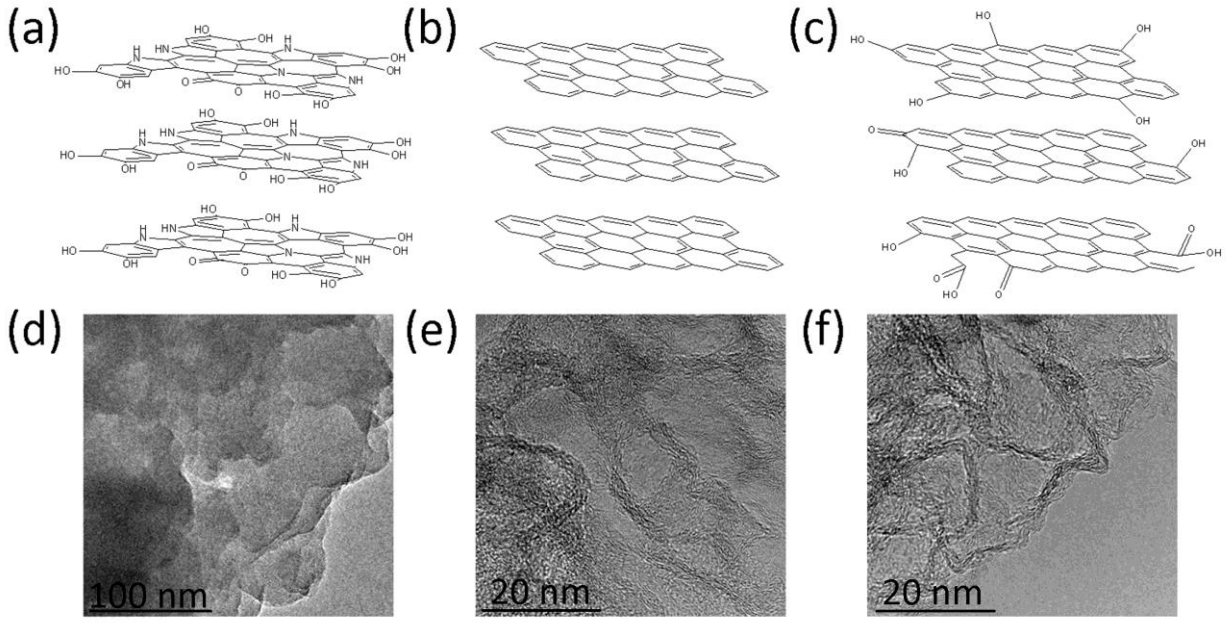


Figure 1 Schematic structure representations (a–c) and TEM images (d–f) of melanin (a, d), GNFs (b, e) and oxidized GNFs (c, f).

Iodinated MB was synthesized by reacting an aqueous solution of MB with acidic solutions of KI and KIO_3 at 100 °C in a closed vial[5] or by grinding samples of solid MB, I_2 and $AgNO_3$ (Figure S1, Supplementary materials) followed by purification of the products on a column filled with silica gel (particle size is 40-63 μm), according to the methods developed for the production of iodinated aromatic compounds.[14]

GNFs were synthesized by pyrolytic decomposition of hexane in the presence of an MgO template at 900 °C for 30 min.[15] GNF surface was oxidized by refluxing with HNO_3 for 1-2 h followed by washing with distilled water. The oxygen groups (predominantly carboxyl and hydroxyl) content in the composition on the surface of oxidized GNFs, according to previously obtained X-ray photoelectron spectroscopy data, was 5.8 at.%.[10] According to the nitrogen isotherm adsorption data, the specific surface area S_{BET} of oxidized GNFs was 126 $m^2 \cdot g^{-1}$, and the pore volume and the pore radius calculated according to the BJH model were 0.451 $cm^3 \cdot g^{-1}$ and 3.64 nm (Figure S2).

To study the adsorption kinetics of MB and I-MB, 0.10 g of oxidized GNFs were placed in 50 mL of aqueous solution of MB or I-MB at the initial concentration of 750 $mg \cdot L^{-1}$. To obtain adsorption isotherms, 10 mL of MB or I-MB solutions with initial concentrations of 0, 15, 30, 45, 60, 90, 120, 150, 350, 500, 750, and 1000 $mg \cdot L^{-1}$ were added to 0.01 g of oxidized GNFs. The residual concentrations of MB and I-MB in the solutions were determined spectrophotometrically at 665 and 443 nm, respectively (Figure S3, Figure S4).

The kinetic curves of MB and I-MB adsorptions on the oxidized GNF surface are presented in Figure 2a. The equilibria in the systems were established within 20 minutes for MB and about 3 h for I-MB. The experimental maximum adsorption capacities Q_{max} for MB and I-MB were 375 and 357 $mg \cdot g^{-1}$ (Figure 2a).

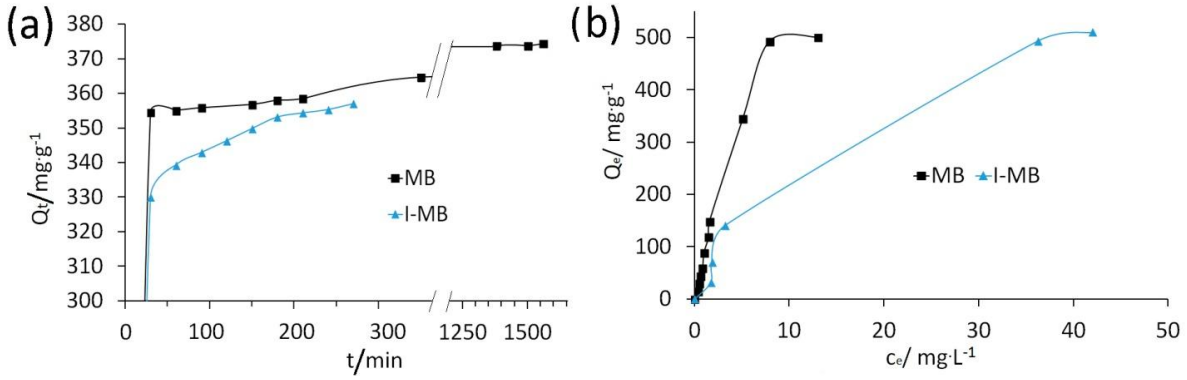


Figure 2 Kinetic (a) and isotherm adsorption (b) curves of MB and I-MB on the oxidized GNF surface.

The kinetic data were processed following the algorithm described for the adsorption of MB on the different carbon surfaces.[12,16-19] The kinetic curves of MB and I-MB adsorptions are shown in the coordination of pseudo-first and pseudo-second orders, the Elovich equation, and the model of intraparticle diffusion (Figure 3). The kinetic equations and the parameters of the corresponding models are presented in Table 1.

Table 1 Models, equations and kinetic parameters of MB and I-MB adsorption on the surface of oxidized GNFs.

Model	Equation in the linear coordinates	Adsorption parameters of MB	Adsorption parameters of I-MB
Pseudo-first order $\frac{dQ_t}{dt} = k_{pl}(Q_e - Q_t)$	$\lg(Q_e - Q_t) = \lg Q_e - \frac{k_1}{2.303}t$	$k_1 = 0.003$ $Q_e = 24.46$	$k_1 = 0.013$ $Q_e = 43.88$
Pseudo-second order $\frac{t}{Q_t} = \frac{1}{k_2 Q_e^2} + \frac{1}{Q_e}t$	$\frac{t}{Q_t} = \frac{1}{k_2 Q_e^2} + \frac{1}{Q_e}t$	$k_2 = 1.33 \cdot 10^{-4}$ $Q_e = 370$	$k_2 = 6.76 \cdot 10^{-4}$ $Q_e = 357$
Elovich equation $q_t = \frac{1}{\beta}\ln(\alpha\beta) + \frac{1}{\beta}\ln t$	$Q_t = \frac{1}{\beta}\ln(\alpha\beta) + \frac{1}{\beta}\ln(t)$	$\alpha = 10.59$ $\beta = 0.2566$	$\alpha = 1.73 \cdot 10^{11}$ $\beta = 0.0811$
Intraparticle diffusion $q_t = k_{id}t^{0.5} + C$	$Q_t = k_{id}t^{0.5} + C$	$k_{id} = 0.53$ $C = 351$	$k_{id} = 2.78/1.24$ $C = 316/336$

Q_t [mg·g^{-1}] is an experimental capacity of oxidized GNFs at the time t. The value of Q_t was calculated using formula $Q_t = \frac{V}{m}(C_0 - C_t)$, where V is solution volume, m is the weight of oxidized GNFs, C_0 and C_t are the concentrations of MB or I-MB in the initial solutions and the measured concentration after adsorption at the time t; Q_e [mg·g^{-1}] is a calculated maximum capacities; k_1 [min^{-1}] and k_2 [(mg·g^{-1})$^{-1}$·min^{-1}] are pseudo-first and pseudo-second orders adsorption rate constants; α [(min·mg·g^{-1})$^{-1}$] is an adsorption constant from Elovich equation; β [g·mg^{-1}] is a degree of surface coverage from Elovich equation; k_{id} [(mg·(g·min)$^{-1}$)$^{-1}$] is an internal diffusion coefficient; C [mg·g^{-1}] is an equilibrium constant in the equation of intraparticle diffusion.

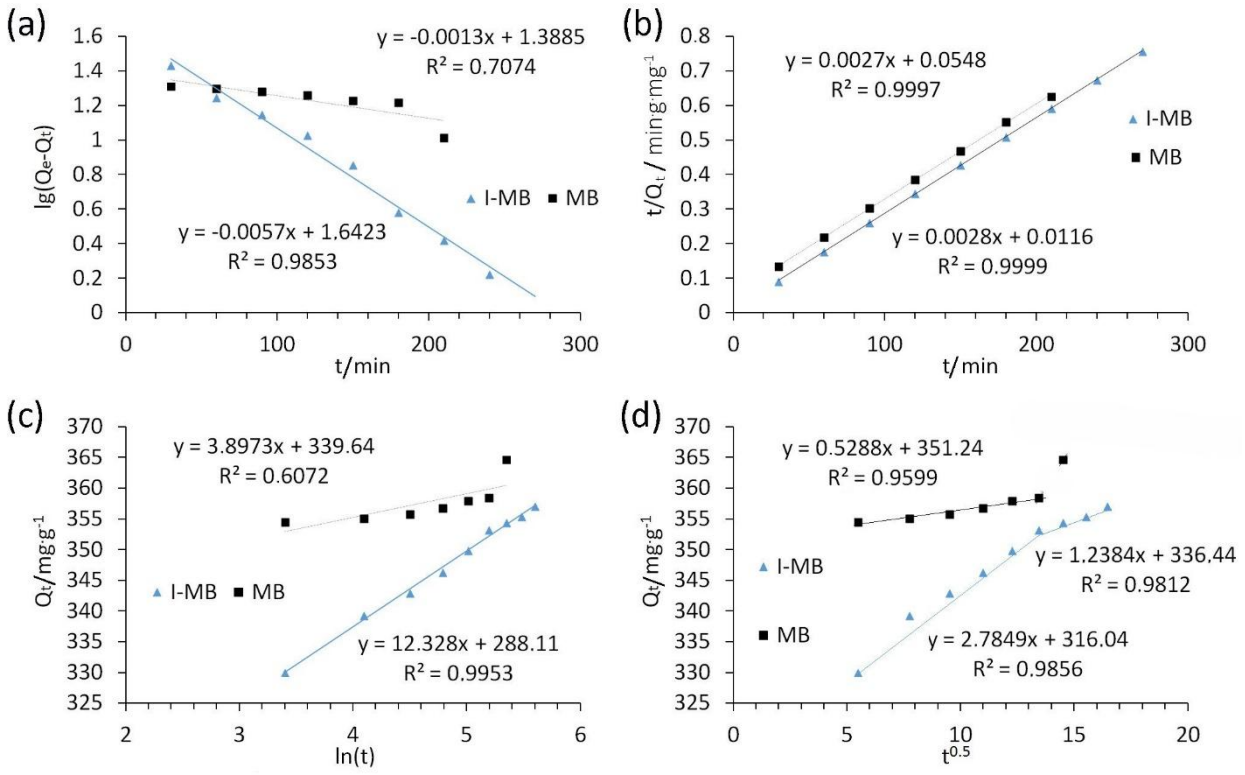


Figure 3 Adsorption kinetic in the linear coordination of pseudo-first (a), pseudo-second (b) orders, Elovich equation (c) and intraparticle diffusion model (d). The linear equations and determination coefficient R^2 are shown in the plots.

The adsorption of MB cannot be satisfactorily described by the pseudo-first order model because of the low determination coefficient $R^2 = 0.7074$ (Figure 3a) that is in accordance with the data.[12,16,17] At the same time, this model is quite satisfactory for I-MB adsorption ($R^2 = 0.9853$). Kinetic curves plotted in pseudo-second order coordinates perfectly describe the adsorption processes of both MB and I-MB (Figure 3b). These results suggest that the adsorption rates may be limited by chemical reactions between MB and I-MB and functional groups on the oxidized GNF surface. The chemisorption model described by the Elovich equation[20] is not suitable for MB

adsorption (R^2 = 0.6072) but satisfies the I-MB adsorption process (R^2 = 0.9953) (Figure 3c). It is likely that in the case of I-MB the adsorption rate is limited by both factors, i.e., the chemical reaction and diffusion of I-MB into the GNF pores, which can be confirmed by the intraparticle diffusion model (Figure 3d). For I-MB the intraparticle diffusion graphs have two linear areas, and none of the lines passes through the point (0; 0) (Figure 3d). The value of the coefficient C of the intraparticle diffusion equation is different from zero (Table 1), indicating a multiple adsorption process.[21] For I-MB, the k_{id} constant decreases almost twice.

Adsorption isotherms and isotherms in the Langmuir and Freindlich coordinates are shown in Figure 2b and Figure 4. The equations and the parameters are presented in Table 2. The impossible negative Q_{max} and k_L values mean that the Langmuir model does not describe the process sufficiently as is also evidenced by low R^2 value (for I-MB, it is 0.7444).[2,12] Thus, Freunlich's model is more consistent. The oxidized GNF surface contains carboxyl and hydroxyl groups with different energies.[10] It can be assumed that the chemisorption process predominantly occurs on the surface of oxidized GNFs. To assess this phenomenon further, MB adsorption was studied on the different adsorbents, i.e., GNFs without functional groups, N-doped GNFs, activated carbon (AC), and SiO_2 (Figure S5). Langmuir's model described the MB adsorption on the surface of the unfunctionalized GNFs, AC and SiO_2 satisfactory but was not suitable for N-doped GNFs (Table S1, Table S2). These results confirm the assumption that chemisorption process dominates over the formation of a monolayer and physical interaction.

Table 2 Freindlich model, equations and isotherm parameters of MB and I-MB adsorption isotherms on the surface of oxidized GNFs.

Model	Equation in the linear coordinate	Adsorption parameters of MB	Adsorption parameters of I-MB
Freindlich model $Q_e = k c_e^{1/n}$	$\ln Q_e = \frac{1}{n}\lg c_e + \lg k$	n = 1.469 k ≈ 103.65	n = 1.398 k ≈ 38.19

n is Freundlich constants; k [mg·g^{-1} (mg^{-1})] shows the adsorption capacity of the sorbent.

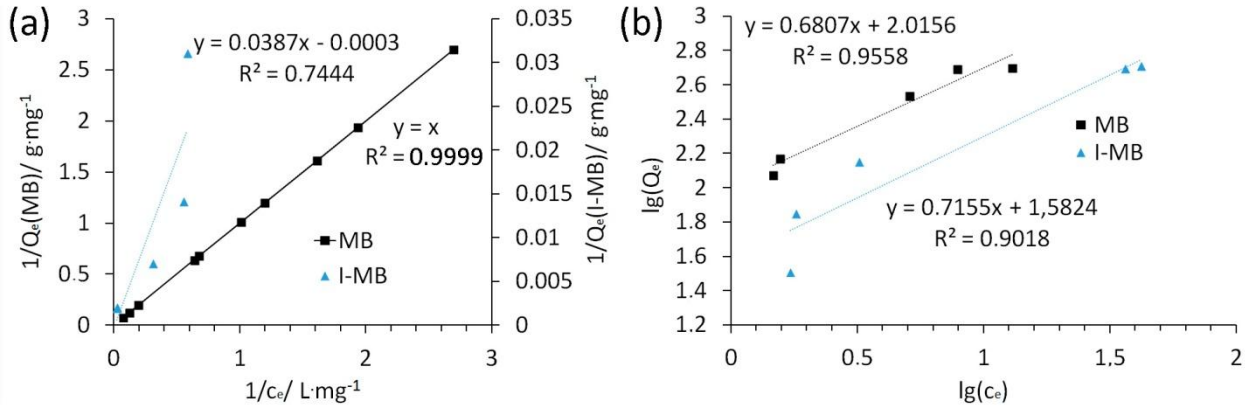


Figure 4 Adsorption isotherm in the liner coordination of Langmuir (a), Freundlich (b) models. The linear equations and determination coefficient R^2 are shown in the plots.

Table 3 contains the calculated specific characteristics of MB and I-MB. The decrease in the number A_m of adsorbed I-MB molecules relative to MB (Table 3) can probably be associated with a change in the electron density in the aromatic system of I-MB as well as with geometry factors. High electronegativity of iodine deactivates the aromatic rings and depletes it of electrons, which worsens the π-π interaction between the I-MB molecule and oxidized GNFs. Another potential factor leading to a decrease in A_m is the large area of the I-MB. The theoretical calculations suggest that the flat MB molecule has an area ~0.04 nm^2 and is located parallel to the plane of the graphene oxide sheet.[12] At the same time, iodine-substituted organic compounds are adsorbed on the carbon surface not flatly.[22]

Table 3 Values of maximum adsorption Q_e, and monolayer capacity A_m, ($\mu mol \cdot m^2$), the area ω_m (nm^2) occupied by MB and I-MB in a dense monolayer.

Adsorbed molecule	M, $g \cdot mol^{-1}$	Q_t,* $mg \cdot g^{-1}$	A_m, $\mu mol \cdot m^{-2}$	ω_m,** nm^2
MB	320	375	9.30	0.18
I-MB	446	357	6.35	0.26

* The Q_t values were extracted from adsorption kinetic curves as a real observed value (Figure 2a).

** The area ω_m was calculated by the formula $\omega_m = \frac{1}{N_A A_m}$, where N_A is Avogadro's number of $6.022 \cdot 10^{23}$ mol^{-1}.

To conclude, the adsorption of MB and I-MB on the GNF surface was studied. The adsorption kinetics of MB can be satisfactorily described by a pseudo-second order model. The adsorption kinetics of I-MB can be described by several models that is in good agreement with the multi-stage nature of adsorption. According to the analysis of isotherm adsorption data, the interaction mechanism between MB and I-MB with GNFs corresponds to chemisorption. A comparison of the values of monolayer capacities A_m and the area ω_m occupied by MB and I-MB in a dense monolayer demonstrates that the adsorption is greater in the case of a geometrically smaller MB molecule. Potentially the iodine atom in the I-MB structure is sterically large, which leads to a larger occupied area in the monolayer. The obtained results open up prospects for using I-MB as a basis for creating selective contrast agents for visualization of melanin-containing tumors by X-ray imaging methods such as computed tomography.

Authors are grateful to Sergey Maximov for help in TEM experiments. The authors are grateful for the support from the MSU Equipment Center “Nanochemistry and Nanomaterials” acting under the Lomonosov Moscow State University Program of Development.

This research was funded by the Russian Science Foundation, grant number 22-15-00072-П.

Online Supplementary Materials

Supplementary data associated with this article can be found in the online version at doi: 10.71267/mencom.8130.

References

1. S. K. Gantsev, M. A. Tatunov, K. S. Gantsev, S. R. Kzyrgalin and R. S. Mukhamedyarov, *Siberian journal of oncology*, 2019, **18(3)**, 71 (in Russian); https://doi.org/10.21294/1814-4861-2019-18-3-71-77.
2. G. Sobal, M. Rodrigues and H. Sinzinger, *Anticancer Res.*, 2008, **28**, 3691; https://ar.iiarjournals.org/content/28/6A/3691
3. E. Link, P. Blower, D. Costa, D. M. Lane, D. Lui, R. S. D. Brown, P. J. Ell and M. F. Spittle, *Eur. J. Nucl. Med.*, 1998, **25**, 1322. https://doi.org/10.1007/s002590050302
4. P. J. Blower, N. J. Carter, *Nucl. Med. Commun.*, 1990, **11**, 413. https://www.ovid.com/00006231-199006000-00003
5. P. V. Shmakova, Y. V. Kutsalo, T. A. Norseev, E. A. Fadeeva, G. E. Krasavin, Y. V. Kodina, V. P. Goltyapin, I. I. Sorokin, I. I Slobodyanik and V. N. Korsunsky, *Medical Radiology and Radiation Safety*, 2002, **47(3)**, 5 (in Russian); https://elibrary.ru/item.asp?edn=mpmexx
6. E. Link, *Monoclonal Antibodies Immunodiagn. Immunother.*, 1999, **18(1)**, 77. https://doi.org/10.1089/hyb.1999.18.77
7. Y. Yin, Y. Jiang, H. Li, W. Yi, F. Li, G. Chen and Z. Wang, *Agric. Prod. Process. Storage*, 2026, **2**, 17. https://doi.org/10.1007/s44462-025-00055-z.
8. W. Song, H. Yang, S. Liu, H. Yu, D. Li, P. Li and R. Xing, *J. Mater. Chem. B*, 2023, **11**, 7528. https://doi.org/10.1039/D3TB01132A
9. L. Tian, X. Li, H. Ji, Q. Yu, M. Yang, L. Guo, L. Huang and W. Gao, *J. Nanobiotechnol.*, 2022, **20**, 485. https://doi.org/10.1186/s12951-022-01698-x
10. E. V. Suslova, M. O. Karimova and S. V. Savilov, *High Energy Chem.*, 2026, 60, 116. https://doi.org/10.1134/S0018143925601095
11. V. Lino, R. Castaldo, G. Gentile and P. Manini, *Mater. Today Sustain.*, 2022, **21**, 100283. https://doi.org/10.1016/j.mtsust.2022.100283.
12. E. Y. Obraztsova, E. S. Bakunin, A. A. Degtyarev, A. V. Rukhov, D. V. Obraztsov, M. S. Goncharova, I. A. Zhabkina and A. V. Trishina, *Mendeleev Commun.*, 2024, **34**, 81. https://doi.org/10.1016/j.mencom.2024.01.024.
13. Z. F. Liu, Z. J. Liu, L. M. Qie and Z. Y. Yao, *Water Conserv. Sci. Eng.*, 2021, **6**, 163. https://doi.org/10.1007/s41101-021-00111-2
14. M. S. Yusubov, E. N. Tveryakova, E. A. Krasnokutskaya, I. A. Perederyna and V. V. Zhdankin, *Synth. Commun.*, 2007, **37(8)**, 1259. https://doi.org/10.1080/00397910701216039
15. S E. V. Suslova, S. V. Yakovlev, K. I. Maslakov, A. V. Desyatov, D. N. Stolbov, D. A. Shashurin, N. N. Kuznetsova and S. V. Savilov, *Mendeleev Commun.*, 2025, **35**, 47. https://doi.org/10.71267/mencom.7531
16. A. H. K. Kadum, I. V. Burakova, E. S. Mkrtchyan, O. A. Ananyeva, V. O. Yarkin, A. E. Burakov and A. G. Tkachev, *Journal of Advanced Materials and Technologies*, 2023, **8(2)**, 130. https://doi.org/10.17277/jamt.2023.02.pp.130-140
17. W. Vallejo, C. Diaz-Uribe, F. Duran, D. P. Vargas-Delgadillo and O. Barbosa, *Sci*, 2025, **7**, 170. https://doi.org/10.3390/sci7040170
18. E. S. Mkrtchyan, E. A. Neskoromnaya, I. V. Burakova, O. A .Ananyeva, N. A. Revyakina, A. V. Babkin, T. S. Kuznetsova, D. A. Kurnosov and A. E. Burakov, *Adv. Mater. Technol.*, 2020, **4**, 21. https://doi.org/10.17277/amt.2020.04.pp.021-028
19. T. D. Khokhlova, G. R. Yunusova and S. N. Lanin, *Russ. J. Phys. Chem. A*, 2018, **95**, 1006. https://doi.org/10.7868/S0044453718050229

20. H. Qiu, L. Lv, B. Pan, Q. Zhang, W. Zhang and Q. Zhang, *J. Zhejiang Univ. Sci., A*, 2009, **10(5)**, 716. https://doi.org/10.1631/jzus.A0820524
21. J. Wang and X. Guo, *Chemosphere*, 2022, **309(2)**, 136732. https://doi.org/10.1016/j.chemosphere.2022.136732
22. S. N. Yashkin, B. A. Murashov and Y. N. Klimochkin, *Russ. J. Phys. Chem.*, 2011, **85**, 677. https://doi.org/10.1134/S0036024411040315

Received: 26th June 2026; Com. 26/8130